JMB

Mutational Analysis and NMR studies of the Death Domain of the Tumor Necrosis Factor Receptor-1

Jean-Baptiste Telliez¹†, Guang-Yi Xu†²*, John D. Woronicz¹, Sang Hsu¹ Jing-Lun Wu¹, Laura Lin², Steven F. Sukits², Robert Powers² and Lih-Ling Lin¹*

¹*Department of Musculoskeletal Science and*

²*Department of Biological Chemistry, Genetics Intitute, Wyeth Research, 87 Cambridge Park Drive, Cambridge MA 02140, USA*

*Corresponding authors

Tumor necrosis factor receptor-1 (TNFR-1) death domain (DD) is the intracellular functional domain responsible for the receptor signaling activities. To understand the transduction mechanism of TNFR-1 signaling we performed structural and functional analysis of the TNFR-DD. The secondary structure of the TNFR-DD shows that it consists of six anti-parallel α-helices. The determination of the topological fold and an extensive mutagenesis analysis revealed that there are two opposite faces that are involved in self-association and interaction with the TRADD death domain. Interestingly, the same critical residues in TNFR-DD are involved in both interactions. There is a good correlation between the binding activities of the mutant proteins and their cytotoxic activities. These results provide important insight into the molecular interactions mediating TNFR-DD self-association and subsequent recruitment of TRADD in the signaling activity of TNFR-1.

© 2000 Academic Press

Keywords: TNFR-1; death domain; mutagenesis; secondary structure; topology

Introduction

Tumor necrosis factor receptor-1 through trimerization induced by the binding of TNFα (cachectin) or TNFβ (lymphotoxin α) trimers elicits a variety of biological responses, including antiviral activity, cytotoxicity, and modulation of gene expression (Beutler & Cerami, 1989; Carswell *et al.*, 1975). TNFα and lymphotoxin α also bind and activate TNFR-2 (Smith *et al.*, 1990). Based on similarities in their cysteine-rich extracellular domains, TNFR-1 and TNFR-2 belong to a receptor superfamily, which besides a number of death inducing receptors, includes CD40 and the low-affinity nerve growth factor receptor (Smith *et al.*, 1994). Although most cell types express both TNF receptors, TNFR-1 appears to play a predominant role in the induction of gene expression and induction

of cell death by TNFα (Tartaglia & Goeddel, 1992; Vandenabeele *et al.*, 1995).

The death domain (DD) was originally described as a region of similarity within the intracellular portions of the TNFR-1 and Fas/Apo1 that is essential for the transduction of cytotoxic signals (Tartaglia *et al.*, 1993). It was subsequently shown that the death domain is a protein interaction motif involved in homo and hetero-association (Boldin *et al.*, 1995). Besides being found in many proteins involved in signaling apoptosis, including receptors and downstream effectors (Ashkenazi & Dixit, 1998; Yuan, 1997), death domains are also present in other proteins that have different cellular functions, such as p75-NGFR, MyD 88, IRAK, MADD, N5, NFκB, DAP kinase, and ankyrins (Feinstein *et al.*, 1995). The solution structure of Fas, FADD, and p75 neurotrophin receptor death domains have recently been determined by NMR spectroscopy (Huang *et al.*, 1996; Jeong *et al.*, 1999; Liepinsh *et al.*, 1997). They consist of six anti-parallel amphipathic α-helices packed into a globular structure. Two other domains called DED (death effector domain) and CARD (caspase recruitment domain) are structurally related to the death domain (Hofmann *et al.*, 1997). Recently, the sol-

---

ution structure of the FADD-DED and RAIDD-CARD were solved, revealing topologies very similar to the known death domain structures (Chou *et al.*, 1998; Eberstadt *et al.*, 1998). Two recent studies have described the three-dimensional structure of Apaf-1 CARD in complex with the procaspase-9 CARD (Qin *et al.*, 1999) and Tube death domain in complex with Pelle death domain (Xiao *et al.*, 1999). These different studies illustrate the diverse association mechanisms in the death domain superfamily.

The low level of sequence conservation between death domains probably reflects their role in diverse cellular functions. Additionally, the apparent absence of a conserved interaction surface suggests that death domains may associate by a variety of mechanisms. Indeed, the surface formed by α-helices 2 and 3 has been implicated in the homo and hetero-association of the death domains of Fas (Huang *et al.*, 1996) and FADD (Jeong *et al.*, 1999). Similar observations have been made in the case of the interaction of the CARD domains of Apaf-1 and procaspase-9 (Day *et al.*, 1999; Qin *et al.*, 1999; Vaughn *et al.*, 1999; Zhou *et al.*, 1999). Conversely, the dimerization of Tube and Pelle death domains seems to rely on contacts between α-helices 4 and 5 of Pelle death domain with α-helix 6 and the unique C-terminal tail of Tube death domain (Xiao *et al.*, 1999). The nature of the interaction also seems to be different between death domain complexes. Electrostatic interactions are thought to be a key component in the interaction between Fas death domain (Fas-DD) and FADD death domain (FADD-DD) (Huang *et al.*, 1996). Whereas, hydrogen bond contacts and van der Waals interactions have been shown to be involved in the complex of Tube and Pelle death domains (Xiao *et al.*, 1999), as well as in the complex of Apaf-1 and procaspase-9 CARD domains (Qin *et al.*, 1999). It is currently thought that the interactions between DEDs are hydrophobic (Eberstadt *et al.*, 1998).

We have assigned the NMR resonance and secondary structure of the human TNFR-1 death domain (TNFR-DD) by NMR spectroscopy and performed mutational studies showing that α2, part of α3 and part of α4 are important for self-association and interaction with TRADD death domain (TRADD-DD).

Results

Structure determination

Structure determination of the wild-type death domain of TNFR-1 by NMR has been hindered due to the low level of protein solubility over a wide range of pH conditions (4-10). Therefore a series of single point mutants has been made and tested for their solubility at different pH conditions. The mutant R347A was found to be soluble and stable in concentrations up to 14 mg/ml (~1 mM) at pH 8.8. Under these conditions the

protein was shown to be predominantly monomeric by size-exclusion chromatography. The HSQC spectrum of ^{15}N-labeled protein indicates that the protein was folded. Therefore, this mutant protein was chosen for the subsequent NMR studies.

However, many of the amide proton peaks were severely broadened due to rapid exchange with water at high pH conditions (pH 8.8), which hindered the complete assignment of TNFR-DD by HSQC-related triple resonance experiments. Nevertheless, the majority of TNFR-DD forms α-helices, where the amide proton exchange is reduced by hydrogen bond formation, allowing for the observation of backbone chemical shifts and the determination of sequential assignments in the helical regions. A total of 63 residues were assigned in the region from A328 to C413, where the amide signals of terminal residues, A316-P327 and G414-R426 were not observed. In an effort to complete the sequential assignment, two experiments were designed based on recently developed methodologies where NMR experiments correlated sequential residues *via* ^{15}N and H$_α$ chemical shifts instead of the amide proton (Kanelis *et al.*, 1998). These experiments enabled us to assign 24 additional residues. Therefore, a total of 87 residues out of 112 amino acid residues were assigned.

Figure 1 summarizes the NMR secondary structure data for TNFR-DD R347A. These data indicate that TNFR-DD consists of six α-helices where helices 1,2,4,5 and 6 exhibit the typical NOE pattern for an α-helix (^3JHN$_α$ < 5 Hz, sequential and medium-range NOEs: $d_{NN}(i,i+1)$, $d_{αN}(i,i+3)$ $d_{αN}(i,i+4)$ and $d_{αβ}(i,i+3)$ and C^α/C^β secondary chemical shifts). These helices are separated by loop regions that were not observed because of the lack of amide proton resonance peaks due to the rapid solvent exchange. C^α/C^β chemical-shift deviation (Figure 1) indicates that both terminal regions are unstructured. A comparison of the secondary structure of TNFR-DD with Fas-DD indicates that the main structural difference between the two proteins resides in the length of helix 3. Helix 3 in the Fas-DD structure encompass nine residues from D240 to E248, whereas in TNFR-DD R347A only three amide protons (E355 to D357) were detectable. The lack of amide peaks in the C terminus region hinders the assignment of the secondary structure for these residues. However, the relatively high amide exchange rate suggests that the structure of this region is somewhat disordered, possibly due to a higher flexibility of helix 3. Data obtained by ^{2}H$_2$O exchange with the mutant R347 K at pH 4 supports this observation (data not shown). Interestingly, similar results were obtained with FADD-DD (Jeong *et al.*, 1999). The two-dimensional helical wheel topology shown in Figure 2 is based on more than 40 long range inter-helical side-chain NOEs assigned from ^{13}C-edited NOESY experiments, combined with secondary structure analysis (Figure 1). TNFR-DD is consistent with other published DD structures
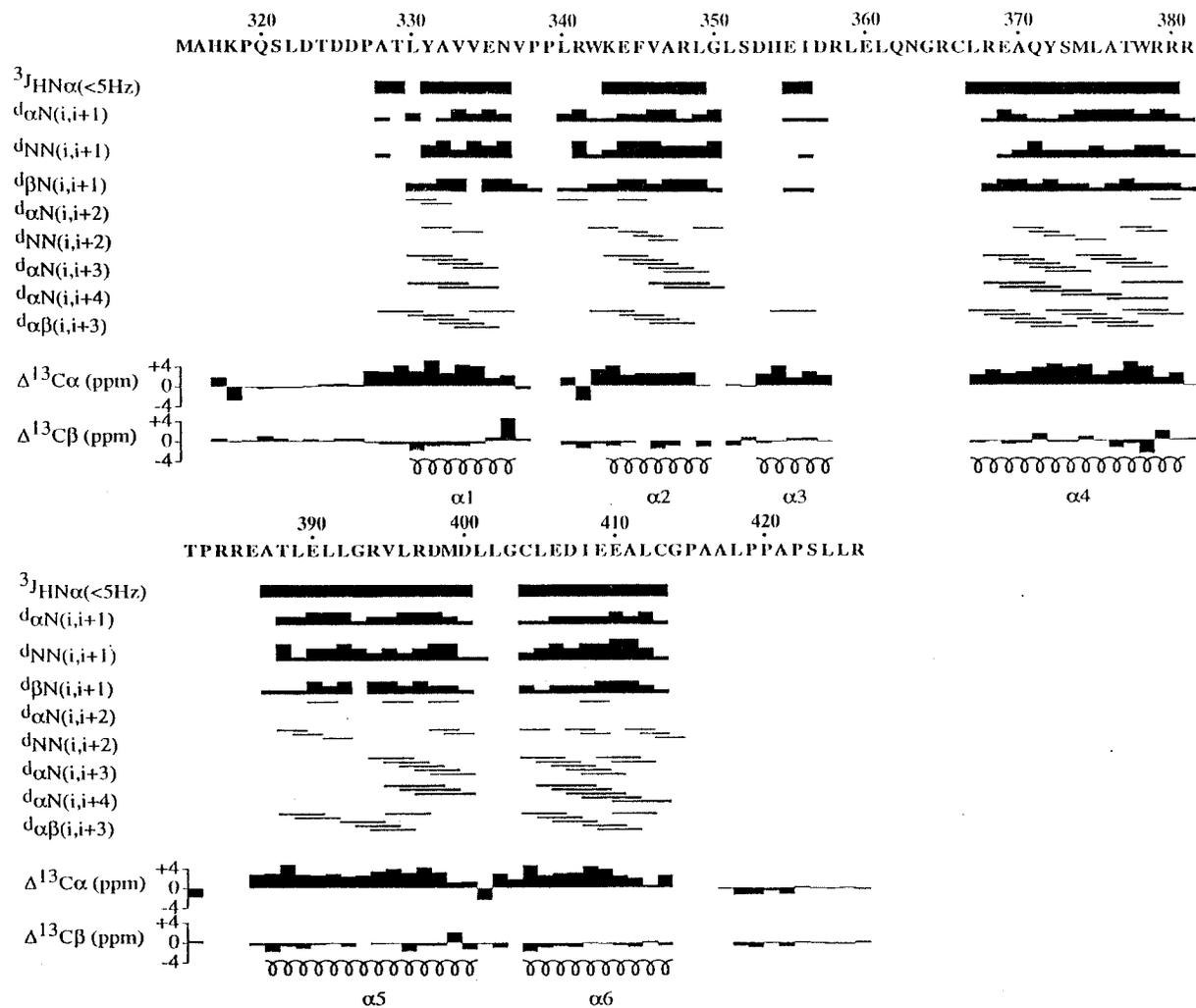
Figure 1. Summary of NMR-derived secondary structure indicators measured for TNFR-DD R347A together with the deduced secondary structure. For NOE data, the thickness of the lines reflects strength of sequential NOEs.

where the protein consists of six α-helices arranged in an anti-parallel fashion. Many of the long range NOEs were found between side-chain residues of α2 making contacts with side-chain residues of α3 (K343-I356, V346-I356, A347-I356), α4 (V346-M374, L349-M374, L349-W378) and α5 (F345-L389, L349-L392, L349-V395, R348-V395). A few NOE pairs involving contacts between α1 and α4 (V334-Q371), as well as between α1 and α6 (V333-I408 and V337-I408), were also found. Only one side-chain contact between α5 and α6 was observed, with L401 at the C terminus of α5 and L405 at the N terminus of α6, suggesting that the angle between these two helices is such that it prevents additional side-chain contacts between them. Based on the planar view centered on helix 2 (Figure 2), helices 2-5 form a twisted four-helix bundle with a hydrophobic core consisting of residues F345, V346, I356, M374, L392. The side-chain of the hydrophilic residues in the helical bundle are solvent exposed. The long-range inter-helical NOEs between side-chain of the residues in the core region indicate that

these residues are close to each other and probably form hydrophobic interactions to stabilize the protein folding.

The secondary structure assignment of R347A is very similar to that of the mutant R347K, which has been shown to have a similar structure to that of the wild-type protein, based on HSQC spectra comparison performed at pH 4.0 (data not shown). Therefore, the overall structure of R347A is most likely similar to that of the wild-type.

Effect of ionic strength on TNFR-DD self-association and its interaction with TRADD-DD

Based on the observation that charged residues have been shown to be involved in the Fas-FADD death domains interaction, we examined the effect of sodium chloride on the TNFR-DD self-association and the interaction with TRADD death domains. Figure 3 shows that increasing concentrations of NaCl are accompanied by a decrease in
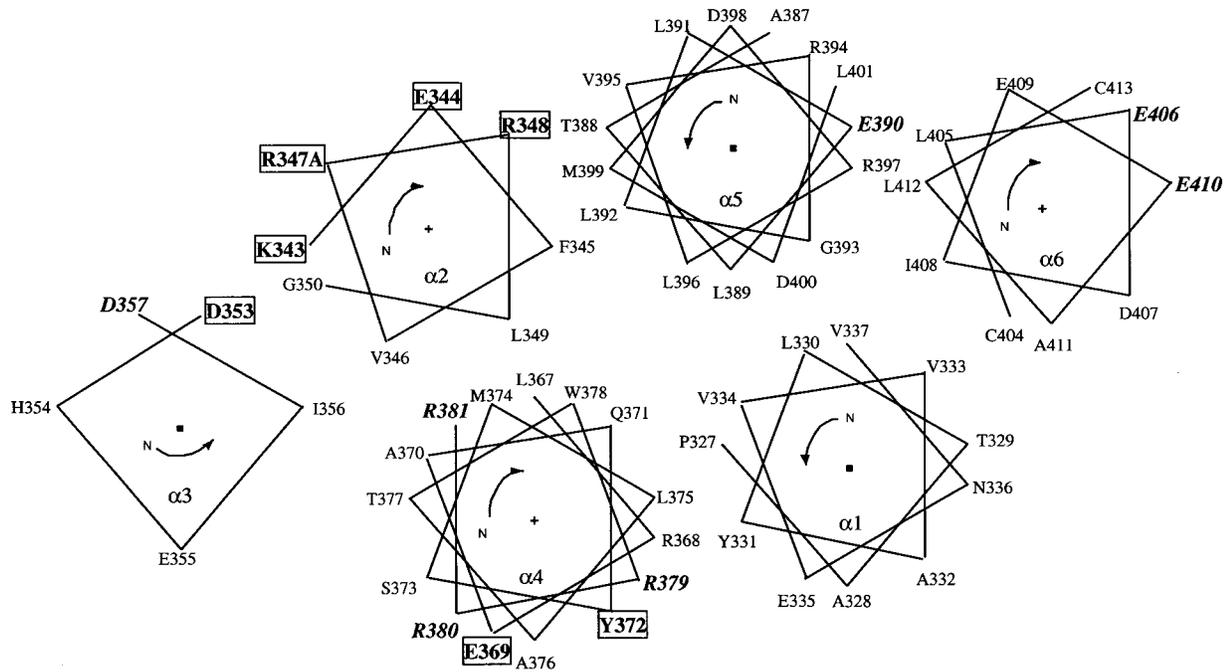
Figure 2. Summary of the inter-helical NOE contacts of TNFR-DD R347A at pH 8.8. The helices 1, 3 and 5 are viewed from their N termini, while helices 2, 4 and 6 are viewed from their C termini. The bold and boxed residues have altered binding properties when mutated to alanine. The bold and italic residues have unaltered binding properties when mutated to alanine (see the text and Figure 5).

death domain interaction in both cases, implying that electrostatic interactions and/or hydrogen bonds are important for the TNFR-DD self-association and its interaction with TRADD-DD.

Effect of TNFR-DD single point mutations on self-association

Since electrostatic interactions might play an important role in death domain interactions, a series of 19 charged amino acid residues were mutagenized (Figure 4). Alanine was chosen as the substituent amino acid, since it eliminates the contribution from the side-chain of the replaced residue with a potential minimal alteration of the overall protein structure. For tyrosine 372 the substitution was made with a phenylalanine in order to abolish the contribution of the hydroxyl group while keeping the aromatic side-chain intact. The wild-type and mutant constructs were expressed in
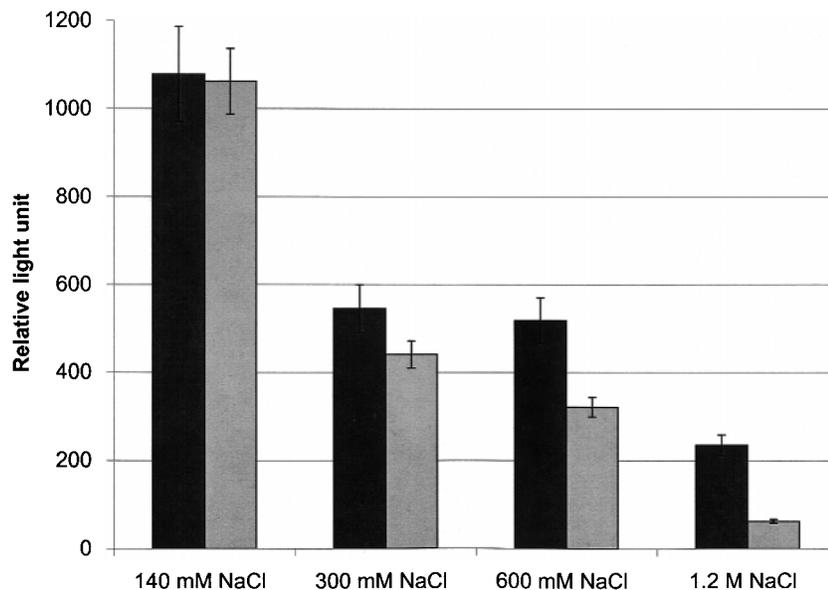

Figure 3. Effect of the ionic strength on the binding of TNFR-DD (200 ng/ml) to MBP-TNFR-DD (dark gray), MBP-TRADD (light gray).
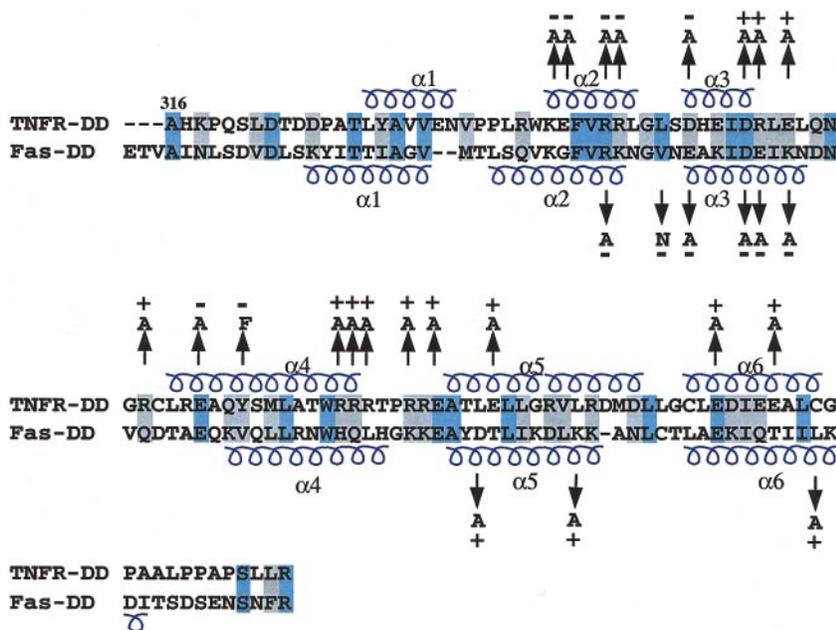
Figure 4. Sequence alignment of the death domains of TNFR-1 and Fas. Identical residues are highlighted in blue and homologous residues in gray. The helices in the NMR structure of the TNFR-1 and Fas (Huang *et al.*, 1996) are indicated. The mutations are indicated by an arrow pointing to the amino acid residue of substitution. A minus sign above the TNFR-1 mutation indicates a loss in self-association or interaction with TRADD-DD (see the text). A minus sign below the Fas mutation indicates that this mutant aggregates less well than the wild-type protein (Huang *et al.*, 1996).

bacteria as His-tagged proteins at the C terminus. The wild-type and most of the mutant proteins were in the insoluble fraction after lysis at pH 7.5. Only mutants E344A and R347A, were soluble upon lysis at pH 7.5. These mutant proteins were purified from the lysate with Ni-NTA resin. All the others, including the wild-type, were extracted directly from the pellet fraction at pH 4.0. The purity of the proteins was determined to be about 80 % by SDS-PAGE. It should be noted that based on the circular dichroism (CD) analysis of the wild-type protein, the helical content appeared to be the same at pH ranging from 4 to 8.8, suggesting that the overall structure of the protein is similar within that pH range, and that the protein is not denatured at pH 4.0 (data not shown).

All the mutants depicted in Figure 4 were studied for their ability to interact with the wild-type death domain in a cell-free binding assay. The wild-type TNFR-DD was expressed as a MBP fusion protein (MBP-TNFR-DD) and was immobilized on 96 well plates for ELISA. Despite the tendency of the wild-type and most of the mutant proteins to aggregate at pH 7.5, all of them were soluble at that pH over the concentration range that was used for these binding experiments (0.1-5 µg/ml). The four mutations K343A, E344A, R347A and R348A in α2 abolish the interaction with the wild-type death domain (Figure 5(a)). Mutation of the first residue of α3, D353A, also abolishes the interaction with the wild-type death domain. Conversely, the next three sequential mutations in α3, D357A, R358A and E360A, and R365A in loop 3 retain an interaction with MBP-TNFR-DD similar to that of the wild-type protein. The first two sequential mutations in α4, E369A and Y372F lost their interaction with the wild-type death domain similar to the mutants in α2. All the

other mutations in α4 (R379A, R380A, R381A), loop 4 (R384A, E386A), α5 (E390A) and α6 (E406A, E410A) retained an interaction with MBP-TNFR-DD similar to that of the wild-type death domain.

Effect of TNFR-DD single point mutations on interaction with TRADD-DD

The TNFR-DD mutants were also studied for their ability to interact with TRADD. The full-length TRADD protein was expressed as a MBP fusion protein (MBP-TRADD) and was immobilized on 96 well plates for ELISA. The trend of the binding ability of all the different mutants to MBP-TRADD is the same as for the binding to MBP-TNFR-DD (Figure 5(b)).

Discussion

We have performed NMR studies and extensive mutagenesis analysis of the TNFR-DD. Overall, the secondary structure of TNFR-DD is similar to the structure of other death domains. It consists of six anti-parallel α-helices. Interestingly, it appears that α2, part of α3 and part of α4 contain important residues for the self-association and interaction with TRADD-DD. A homology model for TNFR-DD was built by utilizing the Fas-DD three-dimensional structure (Huang *et al.*, 1996) (Figure 6). This model of TNFR-DD as well as the two-dimensional helical wheel topology (Figure 2) show that there are two opposite faces involved in TNFR-DD self-association and interaction with TRADD-DD. Individual mutation of the four charged residues in α2, K343A, E344A, R347A and R348A results in a loss of interaction with TNFR-DD and with TRADD-DD. These residues are solvent exposed and located on the same side of the protein, according
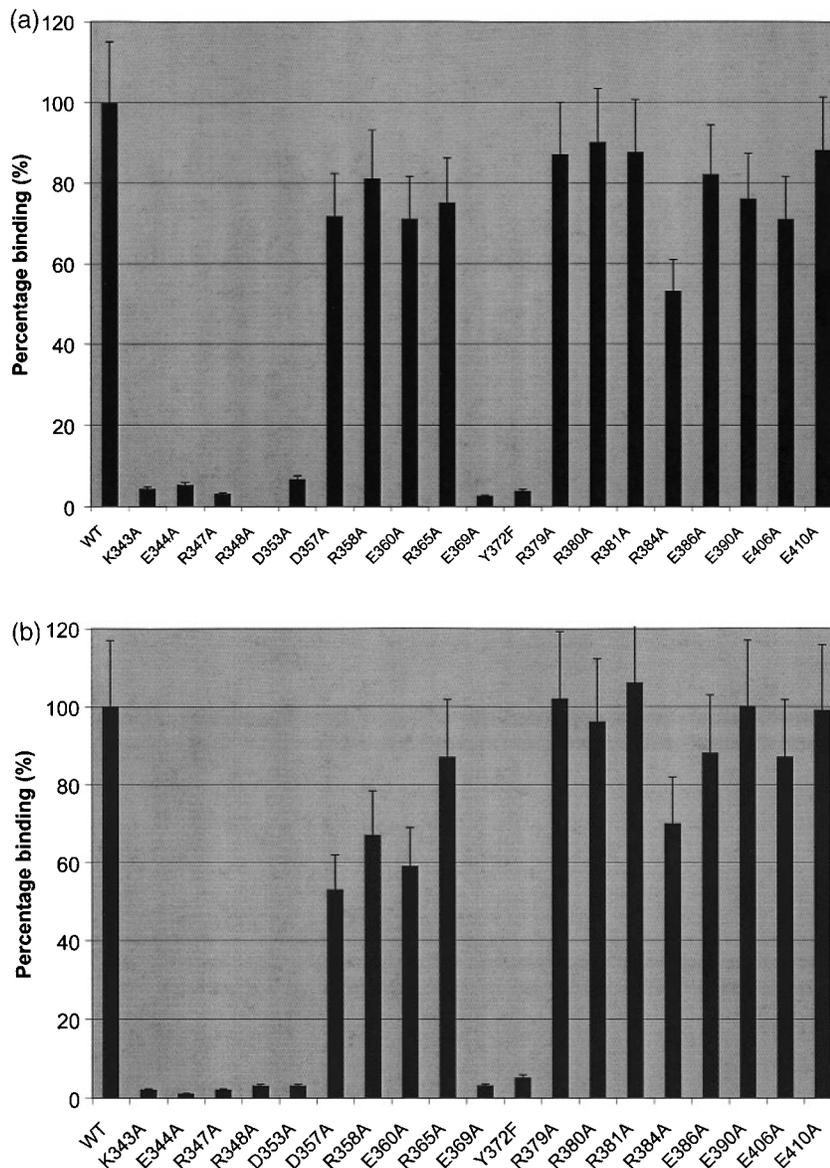
Figure 5. ELISA of TNFR-DD wild-type and mutants binding to MBP-TNFR-DD and MBP-TRADD. (a) Binding of the TNFR-DD mutants to MBP-TNFR-DD immobilized on the plate at 200 ng/well. The reference at 100 % is the binding of the wild-type protein to MBP-TNFR-DD. The values used for the determination of the binding percentage were obtained with ~300 ng/ml of soluble protein. (b) Binding of the TNFR-DD mutants to MBP-TRADD. The experimental conditions used were the same as with MBP-TNFR-DD.

to the deduced topological fold (Figure 2). On the other hand, only the first mutated residue in α3, D353A, has the same effect. The other three mutations in α3 (D357A, R358A and E360A) have no or little effect on the binding properties of the TNFR-DD. In the case of α4, the first two mutants E369A and Y372F are deficient in their interaction with TNFR-DD and TRADD-DD. The other three mutations, R379A, R380A, R381A retain binding properties that are similar to the wild-type protein. The other mutants in loop 3 (R365A), loop 4 (R384A and E386A), α5 (E390A) and α6 (E406A and E410A) also seem to be unaffected in their binding properties when compared to the wild-type protein. These results are in good agreement

with the cytotoxicity data obtained by Tartaglia *et al.* (1993). Mutants R347A and E369A that are defective in our ELISA binding assays are also deficient in cytotoxicity. In contrast, mutants R379A, E390A, E406A and E410A that have unaltered binding properties also retained cytotoxic activity. Only mutant K343A that lost its ability to interact with the wild-type receptor DD or with TRADD-DD retained some cytotoxic activity, also to a lesser extent than the wild-type receptor (Tartaglia *et al.*, 1993). The correlation between death domain interaction and cytotoxicity further supports the hypothesis that the aggregation of TNFR-1 and subsequent recruitment of TRADD through death domain interactions is critical for
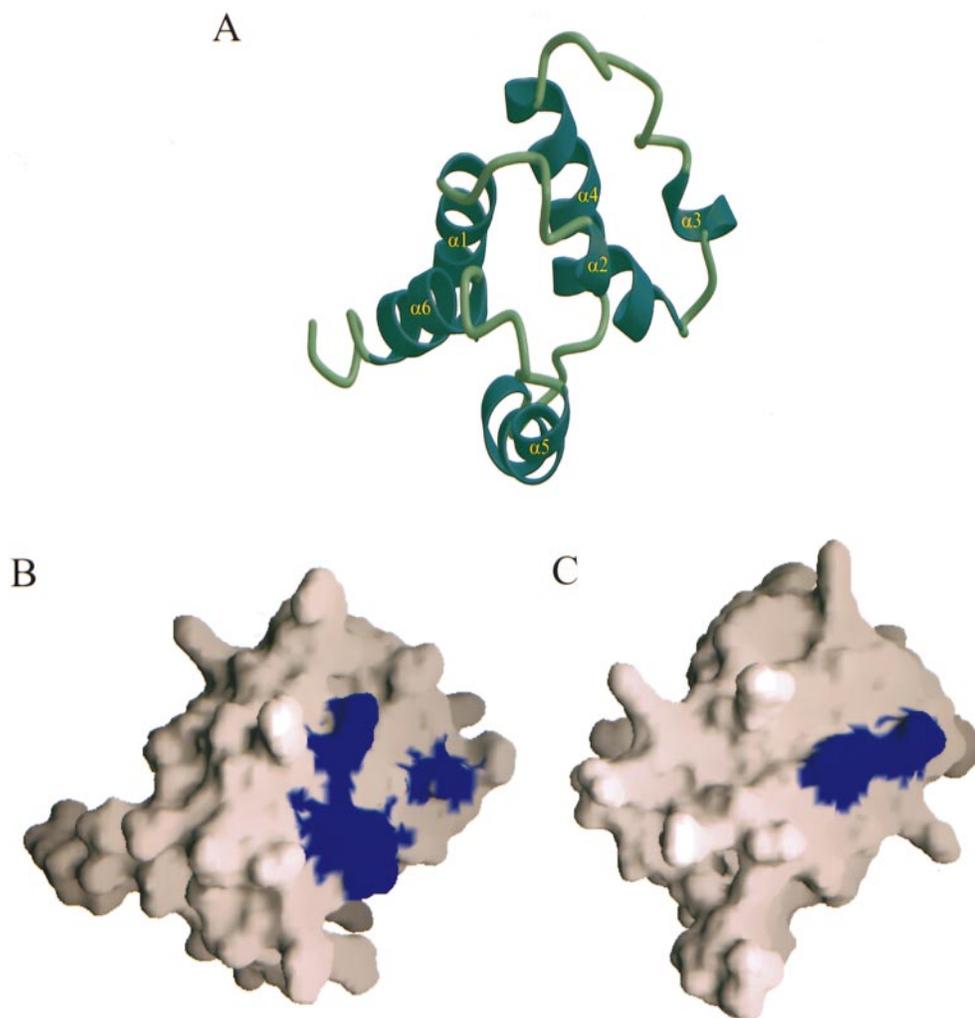
Figure 6. (a) Ribbon diagram of the TNFR-DD homology model based on the sequence alignment with Fas-DD and the observed secondary structure changes by NMR. The α-helices are labeled. (b) A GRASP surface of the TNFR-DD homology model where the residues that affect TNFR-DD self-association and binding to TRADD-DD are blue (same view as (a)). The observed binding surface corresponds to residues in α-helix 2 and 3. (c) A 180° rotation of the GRASP surface in (b), illustrating the second binding surface composed of residues in α-helix 4.

generating a cytotoxic signal (Boldin *et al.*, 1995; Hsu *et al.*, 1995; Vandevoorde *et al.*, 1997). From our results, it is possible that self-association and binding to TRADD-DD use similar surfaces, since all the mutations have the same effect in both cases. When these mutations are placed in the context of the topological fold, it appears that there are two opposite and solvent-exposed faces involved in the interaction. On one side there are critical residues in α2 (K343A, E344A, R347A and R348A) and the beginning of α3 (D353A) and on the other side there are critical residues in α4 (E369A, Y372F). It was recently shown that α2 and α3 of FADD-DD contain critical residues for the interaction with Fas-DD (Jeong *et al.*, 1999). However, the role of α4 in FADD-DD has yet to be addressed.

Interestingly, a comparison of mutations in α3 of Fas and TNFR-1 death domains reveals differences in the contribution of this helix to their respective binding properties. Regarding the self-association, the four mutations in α3 of Fas (E240A, D244A, E245A and K247A) abrogate their self-association (Huang *et al.*, 1996). On the contrary, in the case of TNFR-1, for the four equivalent mutations, only the first one in α3 (D353A) abrogates the interaction with the wild type death domain, as the next three mutations (D357A, R358A and E360A) do not (Figure 4). Therefore, it would seem that the entire helix 3 of Fas-DD is important for the self-association, as in the case of TNFR-DD, only the beginning of helix 3 is important for the self-association. In the case of the Fas-FADD interaction, the first two mutations in α3 of Fas-DD, E240A and D244A greatly affect their interaction with FADD-DD, as the next two mutations E245A and K247A only have a marginal effect. In the case of TNFR-1-TRADD interaction, only the first mutation in α3 of TNFR-DD (D353A) abrogates the interaction with TRADD-DD, as the next three mutations (D357A,

R358A and E360A) do not. It is worth mentioning that while self-association of Fas-DD may not be required for the recruitment of FADD to the receptor, as suggested by the mutants E245A and K247A, we were unable to find mutations in TNFR-DD that have a differential effect on self-association and TRADD binding. Thus, it appears that α3 contains critical residues that can account for the differences between TNFR-1 and Fas regarding their self-association and interaction with other death domain proteins.

The difference between death domain interaction pairs is further demonstrated by the complex of the death domains of Pelle and Tube. The three-dimensional structure of a complex between the death domains of Pelle and Tube was recently published (Xiao *et al.*, 1999). The Tube-Pelle dimers rely on contacts between α4 and α5 of Pelle with α6 and a C-terminal tail of Tube. This is in contrast with the homo and hetero-association of the death domains of TNFR-1 and TRADD, which mainly rely on α2, α3 and α4 of TNFR-1. These results suggest that while a topological fold is maintained between members of the death domain family, the observed selectivity and specificity is obtained by a combination of distinct sequences and surface interpositions between the death domains.

Because of the charged nature of the death domains and the caspase-recruitment domains it was previously proposed that electrostatic interactions might mediate the homotypic interaction (Huang *et al.*, 1996; Jeong *et al.*, 1999). However, the crystal structure of the CARD of Apaf-1 in complex with the CARD of procaspase-9 has been solved, showing that the specificity, as well as the driving force for this interaction, is provided by a combination of extensive hydrogen bond contacts and van der Waals interactions (Qin *et al.*, 1999). Moreover, this interaction is insensitive to high levels of ionic strength, confirming that the driving force of the interaction is not mediated by electrostatic interactions. Similarly, in the case of Pelle and Tube death domains interaction, it has been shown that hydrogen bonds and van der Waals interactions are the driving force for this interaction (Xiao *et al.*, 1999). In the case of TNFR-DD, we have shown that interaction with the wild-type death domain and interaction with TRADD-DD is disrupted at high levels of salt concentration (0.3 M-1.2 M). These results suggest that TNFR-DD interactions are mediated, at least in part, by electrostatic interactions, similarly to that shown in the case of Fas-DD (Huang *et al.*, 1996). This is also supported by our mutagenesis study in which mutation of many of the charged residues to alanine induces a loss of self-interaction or interaction with TRADD-DD. These different studies show that not only the surfaces, but also the nature of the interactions involved in death domain associations are not conserved, which provides for a mechanism of death domain selectivity and specificity of interaction.

In TNFR-1 signaling, the receptor trimerizes upon binding with a TNF trimer and then recruits TRADD. Our experiments show that the critical residues for TNFR-DD self-association or interaction with TRADD-DD are the same. Therefore, it is possible that self-association of TNFR-DD and interaction with TRADD-DD occurs *via* the same binding surface. If this is the case, it is possible that ligand-induced trimerization of the receptor recruits TRADD by simply increasing the level of affinity for TRADD due to an increase in the local concentration of TNFR-DD. Alternatively, TNFR-1 trimerization may create a high-affinity binding site for TRADD. It is also possible that a third partner is involved in the regulation of the recruitment of TRADD to TNFR-1; Recently, SODD was shown to be constitutively bound to TNFR-1 intracellular domain and released from the receptor upon binding of the ligand, allowing for TRADD to be recruited to TNFR-1 (Jiang *et al.*, 1999). It is possible that SODD prevents TRADD from interacting with TNFR-1 in the absence of ligand bound to the receptor.

In conclusion, TNFR-DD consists of six anti-parallel α-helices similar to other death domains where the major structural and functional difference occurs in α3. Based on the current mutagenesis study, helices α2 and part of α3 constitute a binding surface on one side of the protein, while α4 constitutes another binding surface on the opposite side of the protein. The critical residues involved in self-association as well as interaction with TRADD-DD are the same, suggesting a very similar mode of interaction in both cases.

Materials and Methods

TNFR-DD cloning and site-directed mutagenesis

The DNA sequence coding from residue A316 to R426 from hTNFR-1 was cloned in pRSETB (Invitrogen) after amplification by PCR. The primer at the 5′ end introduces an initiation site with an *Nde*I site upstream of the methionine residue, and the primer at the 3′ end introduces a His-tag after R426. The sequence was confirmed by sequencing. Single point mutations were introduced using chameleon double-stranded site-directed mutagenesis (Stratagene) and verified by sequencing of the coding region.

Preparation of R347A mutant for NMR studies

Samples of 20 g of wet cell paste expressing TNFR-DD R347A were resuspended in 300 ml of lysis buffer containing 50 mM Tris-HCl (pH 8.8), 50 mM NaCl, and protease inhibitor tablets (Boehringer Mnnheim GmbH, Mannheim, Germany). Cells were lysed by two passages through a Microfluidizer (Microfluidics Corporation, Newton, MA). Cellular debris were removed by centrifugation at 15,000 *g* for 30 minutes. The soluble extract was then loaded onto a 2 cm × 20 cm Ni-NTA Superflow (Qiagen) column pre-equilibrated with lysis buffer. The column was washed with a large amount of lysis buffer until no protein was present in the flow-through, as judged by Bradford protein assay. TNFR-DD R347A

was eluted with a step elution of 400 mM imidazole in lysis buffer. DTT was added immediately to the eluate to a final concentration of 10 mM. Death domain-containing fractions were pooled and dialysed against buffer A (50 mM Tris-HCl (pH 8.8), 50 imidazole, 10 mM DTT) overnight, and applied onto a 1 cm × 10 cm Toyopearl QAE-550C anion exchange column (TosoHaas, Montgomeryville, PA) pre-equilibrated with buffer A. Greater than 95 % (w/w) pure R347A mutant was eluted with a linear NaCl gradient. The fractions were subjected to SDS-PAGE analysis and good fractions were combined and concentrated before loading onto a Superdex 75 gel filtration column (Amersham Pharmacia Biotech, Piscataway, NJ) equilibrated with buffer containing 50 mM Tris-HCl (pH 8.8), 100 mM NaCl, 50 mM Imidazole, 10 mM DTT. R347A-containing fractions were eluted, dialysed and concentrated for NMR studies.

NMR spectroscopy

All NMR spectra were acquired at 25 °C on Varian Unity+ 600 MHz spectrometer. A series of HSQC (Muhandiram & Kay, 1994) related three-dimensional triple-resonance experiments were recorded using uniformly ^{15}N and $^{15}N/^{13}C$-labeled protein in water with 5 % ^2H_2O, including HNCO, (HB)CBCACONNH, HNCACB, C(CC)_TOCSY_(CO)NNH, H(CC)_TOCSY_(CO)NNH, and HAHB(CBCA)CONNH, and HN(CACB)-HAHB experiments (Kay, 1995; Muhandiram & Kay, 1994) to make backbone, side-chain and sequential assignments. 3D-HNHA (Garrett et al., 1994) and 2D HMQC-J (Kay & Bax, 1990) were carried out for $^3J_{NH\alpha}$ coupling constant measurement. R347A is a proline-rich protein that contains a total of nine proline residues. The HBCBCA(CO)_N_CAHA and HACA_N (Kanelis et al., 1998), which correlates sequential residues *via* their ^{15}N nuclei, were used to assign these proline residues and additional amide residues missing, due to fast exchange with water at pH 8.8. Validation and additional residue assignments were made using both ^{15}N-edited NOESY and ^{13}C-edited NOESY experiments (Pascal et al., 1994; Xu et al., 1995). Data sets were processed and displayed on SGI work station using the programs NMRDraw and NMRPipe (Delaglio et al., 1995). The programs PIPP and STAPP (Garrett et al., 1991) were used for peak picking, data analysis and part of auto-sequential assignment.

TNFR-DD three-dimensional structural model

The TNFR-DD sequence alignment with Fas-DD was determined using QUANTA98 (Molecular Simulations, Inc. San Diego, CA). An initial homology model for TNFR-DD based on its sequence alignment with Fas-DD was accomplished with MODELLER (Sali et al., 1995; Sanchez & Sali, 1998). The TNFR-DD homology model was further refined to maintain consistency with the observed secondary structure elements observed by NMR. Basically, the structure was subjected to a simulated annealing protocol (Nilges et al., 1988) using the program XPLOR (Brünger, 1993) where only regions of the protein that differed from the secondary structure observed by NMR were free to move. φ and ψ dihedral constraints based on accepted values for standard secondary structure elements were applied to residues identified to be α-helical by NMR, otherwise no constraints were applied and the residue was free to move. The Fas-DD sequence and solution structure (PDB acces-

sion code 1DDF) were used as reported by Huang et al. (1996).

Protein preparation for binding assay

Wild-type and mutant recombinant TNFR-DD proteins were prepared from *Escherichia coli* strain BL21 (DE3) pLysS (Stratagene). When cell growth reached an absorbance at 595 nm of ~0.5 at room temperature, protein expression was induced by adding 0.3 mM isopropyl-1-thio-β-D-galactopyranoside for four hours. Cells were lysed with the French press (1000 psi) in 50 mM Tris (pH 7.5), 50 mM NaCl, 10 µg/ml leupeptin, 10 µg/ml aprotinin 2 mM phenylmethylsulfonyl fluoride at 4 °C. The lysate was centrifuged at 21,000 *g* at 4 °C for 30 minutes. The soluble mutants were then incubated for one hour with Ni-NTA resin (Qiagen) at 4 °C. The resin was washed twice in 50 mM Tris (pH 7.5), 50 mM NaCl and twice in 50 mM Tris (pH 7.5), 50 mM NaCl, 50 mM imidazole. The bound protein was eluted from the resin in 50 mM Tris (pH 7.5), 50 mM NaCl, 250 mM imidazole and 10 mM DTT was added to the eluate. The wild-type protein and most of the mutants were in the pellet fraction after lysis. The pellet was then washed twice in 50 mM Tris (pH 8.5), 50 mM NaCl and the death domain proteins were extracted in 50 mM NaOAc (pH 4.0), 50 mM $MgSO_4$. Aliquots of 10 mM DTT was then added to the extract.

Effect of ionic strength on TNFR-DD self-association and association with TRADD-DD

The experiments were carried out according to the protocol described below (TNFR-DD binding assay). Only, the binding buffer was supplemented with NaCl 5 M to obtain the desired final concentrations of 140 mM, 300 mM, 600 mM and 1.2 M.

TNFR-DD binding assay

TNFR-DD binding to itself or to TRADD was determined by an enzyme-linked immunosorbent assay (ELISA). A total of 96 well plates were coated overnight at 4 °C with 200 ng MBP-TNFR-DD, MBP-TRADD or MBP-MADD-LZ (N-terminal region of MADD containing a leucine zipper motif) in coating buffer (25 mM Mops (pH 7.5), 150 mM NaCl, 10 mM DTT, 0.02 % (w/w) NaN_3). The plates were then incubated in blocking buffer (10 mM Mops (pH 7.5), 150 mM NaCl, 0.05 % (w/w) Tween 20, 0.1 % (w/w) Gelatin, 0.02 % (w/w) NaN_3) for one hour followed by a one hour incubation with the different TNFR-DD proteins in binding buffer (100 mM Tris (pH 7.5), 140 mM NaCl, 0.1 mM EDTA, 0.2 % (w/w) Triton X-100, 10 mM DTT). The plates were washed four times in 10 mM K_2PO_4 (pH 7.4), 0.05 % Tween 20. The bound His tagged proteins were then incubated for 30 minutes in 10 mM Mops (pH 7.5), 150 mM NaCl, 0.05 % Tween 20, 0.02 % NaN_3, anti-6x His mAb (1:1000), anti-mouse Biotin (1:1000), Streptavidin-Alkaline Phosphatase (1:1000). The plates were washed four times in 10 mM K_2PO_4 (pH 7.4), 0.05 % Tween 20. Tropix CDP-Star/Sapphire II solution was used for the luminescent reaction and detection with the lumicount plate reader (Packard).

Acknowledgments

References

Ashkenazi, A. & Dixit, V. M. (1998). Death receptors: signaling and modulation. *Science,* **281**, 1305-1308.

Beutler, B. & Cerami, A. (1989). The biology of cachectin/TNF – a primary mediator of the host response. *Annu. Rev. Immunol.* **7**, 625-655.

Boldin, M. P., Mett, I. L., Varfolomeev, E. E., Chumakov, I., Shemer-Avni, Y., Camonis, J. H. & Wallach, D. (1995). Self-association of the ''death domains'' of the p55 tumor necrosis factor (TNF) receptor and Fas/APO1 prompts signaling for TNF and Fas/APO1 effects. *J. Biol. Chem.* **270**, 387-391.

Brünger, A. T. (1993). *X-PLOR Version 3.1 Manual*, Yale University, New Haven, USA, CT.

Carswell, E. A., Old, L. J., Kassel, R. L., Green, S., Fiore, N. & Williamson, B. (1975). An endotoxin-induced serum factor that causes necrosis of tumors. *Proc. Natl Acad. Sci. USA,* **72**, 3666-3670.

Chou, J., Matsuo, H., Duan, H. & Wagner, G. (1998). Solution structure of the RAIDD CARD and model for CARD/CARD interaction in caspase-2 and caspase-9 recruitment. *Cell,* **94**, 171-180.

Day, C. L., Dupont, C., Lackmann, M., Vaux, D. L. & Hind, M. G. (1999). Solution structure and mutagenesis of the caspase recruitment domain (CARD) from Apaf-1. *Cell Death Differ.* **6**, 1125-1132.

Delaglio, F., Grzesiek, S., Vuister, G. W., Zhu, G., Pfeifer, J. & Bax, A. (1995). NMRPipe: a multidimensional spectral processing system based on UNIX pipes. *J. Biomol. NMR,* **6**, 277-293.

Eberstadt, M., Huang, B., Chen, Z., Meadows, R. P., Ng, S. C., Zheng, L., Lenardo, M. J. & Fesik, S. W. (1998). NMR structure and mutagenesis of the FADD (Mort1) death-effector domain. *Nature,* **392**, 941-945.

Feinstein, E., Kimchi, A., Wallach, D., Boldin, M. & Varfolomee, E. (1995). The death domain: a module shared by proteins with diverse cellular functions. *Trends Biochem. Sci.* **20**, 342-344.

Garrett, D. S., Kuszewski, J., Hancoca, T. J., Lodi, P. J., Vuister, G. W., Gronenborn, A. M. & Clore, G. M. (1994). The impact of direct refinement against three-bond HN-C$^{\alpha}$H coupling constants on protein structure determination by NMR. *J. Magnet. Reson.* **104**, 99-103.

Garrett, D. S., Powers, R., Gronenborn, A. M. & Clore, G. M. (1991). A common sense approach to peak picking in two, three, and four dimensional spectra using automatic computer analysis of contour diagrams. *J. Magnet. Reson.* **95**, 214-220.

Hofmann, K., Bucher, P. & Tschopp, J. (1997). The CARD domain: a new apoptotic signalling motif. *Trends Biochem. Sci.* **22**, 155-156.

Hsu, H., Xiong, J. & Goeddel, D. V. (1995). The TNF receptor 1-associated protein TRADD signals cell death and NF-kappa B activation. *Cell,* **81**, 495-504.

Huang, B., Eberstadt, M., Olejniczak, E. T., Meadows, R. P. & Fesik, S. W. (1996). NMR structure and mutagenesis of the Fas (APO-1/CD95) death domain. *Nature,* **384**, 638-641.

Jeong, E.-J., Bang, S., Lee, T. H., Park, Y. I., Sim, W.-S. & Kim, K.-S. (1999). The solution structure of FADD death domain. *J. Biol. Chem.* **274**, 16337-16342.

Jiang, Y., Woronicz, J. D., Liu, W. & Goeddel, D. V. (1999). Prevention of constitutive TNF receptor 1 signaling by silencer of death domains. *Science,* **283**, 543-546.

Kanelis, V., Farrow, N. A., Kay, L. E., Rotin, D. & Forman-Kay, J. D. (1998). NMR studies of tandem WW domains of Nedd4 in complex with a PY motif-containing region of the epithelial sodium channel. *Biochem. Cell Biol.* **76**, 341-350.

Kay, L. E. (1995). Pulsed field gradient multi-dimensional NMR methods for the study of protein structure and dynamics in solution. *Prog. Biophys. Mol. Biol.* **63**, 277-299.

Kay, L. E. & Bax, A. (1990). New methods for the measurement of NH-C$^{\alpha}$H coupling constants in ^{15}N labeled proteins. *J. Magn. Reson.* **86**, 110-126.

Liepinsh, E., Ilag, L. L., Otting, G. & Ibanez, C. (1997). NMR structure of the death domain of the p75 neurotrophin receptor. *EMBO J.* **16**, 4999-5005.

Muhandiram, D. R. & Kay, L. E. (1994). Gradient enhanced triple-resonance three dimensional NMR experiments with improved sensitivity. *J. Magnet. Reson.* **103**, 203-216.

Nilges, M., Gronenborn, A. M., Bruenger, A. T. & Clore, G. M. (1988). Determination of three-dimensional structures of proteins by simulated annealing with interproton distance restraints. Application to crambin, potato carboxypeptidase inhibitor and barley serine proteinase inhibitor 2. *Protein Eng.* **2**, 27-38.

Pascal, S. M., Muhandiram, D. R., Yamazaki, T., Forman-Kay, J. D. & Kay, L. E. (1994). Nuclear magnetic resonance structure of an SH2 domain of phospholipase C-gamma 1 complexed with a high affinity binding peptide. *J. Magnet. Reson.* **103**, 197-201.

Qin, H., Srinivasula, S. M., Wu, G., Fernandes-Alnemri, T., Alnemri, E. S. & Shi, Y. (1999). Structural basis of procaspase-9 recruitment by the apoptotic protease-activating factor 1. *Nature,* **399**, 549-557.

Sali, A., Potterton, L., Yuan, F., van Vlijmen, H. & Karplus, M. (1995). Evaluation of comparative protein modeling by MODELLER. *Proteins: Struct. Funct. Genet.* **23**, 318-326.

Sanchez, R. & Sali, A. (1998). Evaluation of comparative protein structure modeling by MODELLER-3. *Proteins: Struct. Funct. Genet.* **Suppl. 1**, 50-58.

Smith, C. A., Davis, T., Anderson, D., Solam, L., Beckmann, M. P., Jerzy, R., Dower, S. K., Cosman, D. & Goodwin, R. G. (1990). A receptor for tumor necrosis factor defines an unusual family of cellular and viral proteins. *Science,* **48**, 1019-1023.

Smith, C. A., Farrah, T. & Goodwin, R. G. (1994). The TNF receptor superfamily of cellular and viral proteins: activation, costimulation, and death. *Cell,* **76**, 959-962.

Tartaglia, L. A., Ayres, T. M., Wong, G. H. W. & Goeddel, D. V. (1993). A novel domain within the 55 kd TNF receptor signals cell death. *Cell,* **74**, 845-853.

Tartaglia, L. A. & Goeddel, D. V. (1992). Two TNF receptors. *Immunol. Today,* **13**, 151-153.

Vandenabeele, P., Declercq, W., Beyart, R. & Fiers, W. (1995). Two tumor necrosis factor receptors: structure and function. *Trends Cell Biol.* **5**, 392-399.

Vandevoorde, V., Haegeman, G. & Fiers, W. (1997). Induced expression of trimerized intracellular domains of the human tumor necrosis factor (TNF) p55 receptor elicits TNF effects. *J. Cell Biol.* **137**, 1627-1638.

Vaughn, D. E., Rodriguez, J., Lazebnik, Y. & Joshua-Tor, L. (1999). Crystal structure of Apaf-1 caspase recruitment domain: an α-helical greek key fold for apoptotic signaling. *J. Mol. Biol.* **296**, 937-947.

Xiao, T., Towb, P., Wasserman, S. A. & Sprang, S. R. (1999). Three-dimensional structure of a complex between the death domains of pelle and tube. *Cell,* **99**, 545-555.

Xu, G. Y., Ong, E., Gilkes, N. R., Kilburn, D. G., Muhandiram, D. R., Harris-Brandts, M., Carver, J. P., Kay, L. E. & Harvey, T. S. (1995). Solution structure of a cellulose-binding domain from *Cellulomonas fimi* by nuclear magnetic resonance spectroscopy. *Biochemistry,* **34**, 6993-7003.

Yuan, J. (1997). Transducing signals of life and death. *Curr. Opin. Cell. Biol.* **9**, 247-251.

Zhou, P., Chou, J., Olea, R. S., Yuan, J. & Wagner, G. (1999). Solution structure of Apaf-1 CARD and its interaction with caspase-9 CARD: a structural basis for specific adaptor/caspase interaction. *Proc. Natl Acad. Sci. USA,* **96**, 11265-11270.